# **Original Research**



# Spatiotemporal Ca<sup>2+</sup> dynamics in neuronal dendrites: responses and support of travelling waves

Nicolangelo Iannella<sup>1,\*</sup>, Roman R. Poznanski<sup>2</sup>

<sup>1</sup>The Faculty of Mathematics and Natural Sciences, University of Oslo, Oslo 0316 Norway

\*Corresponding author: n.l.iannella@ibv.uio.no DOI:https://doi.org/10.56280/1714100811

This article is an open-access article distributed under the terms and conditions of the Creative Commons Attributions (CC BY) license (https://creativecommons.org/licenses/by/4.0/)

Received: 13 July 2025 Accepted: 21 September 2025 Online published 29 September 2025

#### **Abstract**

Since the onset of intracellular voltage recording techniques, additional methods have been developed and improved upon, such as using voltage-activated dyes, sodium indicators, fluorescent proteins (namely Green fluorescent protein (GFP)), synthetic and genetically encoded indicators, in conjunction with calcium imaging. These techniques have shown that dendrites are not just simple transmission lines, but are sophisticated cellular systems with nonlinear multiscale dynamics that evolve over different timescales and are involved in neural signalling, information processing, along with any underlying computations. Calcium imaging has been important in this regard, having highlighted how reaction-diffusion processes between calcium, buffers and other proteins shape neuronal activity, through dynamical interaction and synaptic plasticity, over different timescales compared to the evolution of electrical signals. To this end, experiments have shown the involvement of calcium and calcium dependent buffers in the response dynamics of neurons. A novel participant during morphological studies, using electron microscopy, fluorescence and immunostaining have illustrated that the Endoplasmic Reticulum (ER) (present in the soma and extends into the distal dendrites) is also a calcium store that can release calcium as puffs through the activation ryanodine receptors into the cytosol of neuronal dendrites. This is called  $Ca^{2+}$ -induced  $Ca^{2+}$  release (CICR), which have been implicated in a number of processes, including the occurrence of calcium waves in the presence of a unsaturated buffer. In this situation, one can observe local changes to the  $Ca^{2+}$  and buffer concentrations in response to some stimuli, such as the presentation of orientated stationary or moving bars or gratings, in a selective fashion through the manifestation of a bias in the resulting calcium concentration in space along the dendrite, that underpins some computation. Studies have shown that  $Ca^{2+}$  plays many important roles in neuronal function and information processing. To better understand the role of  $Ca^{2+}$ , we constructed a computational model of a dendrite with a mechanism that describes CICR in the presence of an unsaturated buffer and study the conditions permitting the occurrence calcium waves and the underlying requirements of timed inputs from CICR. Modeling the heterogeneity of CICR from the endoplasmic reticulum by using a formulation that permits essential dynamics to be analyzed. Using a two-pool model calcium dynamics, we present an analysis of how CICR impacts calcium activity in space in the presence of a calcium buffer and study the potential conditions supporting the propagation of CICR induced  $Ca^{2+}$  waves.

*Keywords:* Endoplasmic reticulum, Calcium ions, Calcium-Induced-Calcium Release mechanism, Two-pool calcium model.

# 1. Introduction

Selective neural responses, such as orientation and direction selectivity, have been demonstrated in many published papers that have used different mammals, such as cat, monkey, and ferret. Upon

presentation of some preferred stimuli, neurons show vigorous responses while to non preferred stimuli, the responses are markedly weaker or lacking. The first demonstrated example of selective neural responses was orientation selectivity

J. Multisc. Neurosci. Vol.4(3), 208-220 (©2025 The Authors) Published by Neural Press

<sup>&</sup>lt;sup>2</sup>Integrative Neuroscience Initiative, Melbourne Australia 3145

where cortical neurons responded strongly to the presentation of visual stimuli composed of bars at some preferred orientation (Blasdel, 1992; Heggelund & Moors, 1983; Martinez et al., 2002; Merkulyeva et al., 2025; Murphy & Sillito, 1986; Scholl et al., 2013; Volgushev et al., 1993), which was followed by illustrating direction selectivity in cortical neurons of the early visual cortex (Barlow et al., 1964; Barlow & Levick, 1965; Bonhoeffer & Grinvald, 1993; Gizzi et al., 1990; Movshon, 1975).

To this end, the strong selective responses of retinal ganglion cells were shown to be *direction-selective*, responding maximally to stimuli moving in the cells' preferred direction (Barlow et al., 1964; Barlow & Levick, 1965), and can be attributed to the spatial extent of the dendrite and the timing and patterning of input, as an underlying mechanism. For starburst amacrine cells (SAC) Euler et al. (2002) has further demonstrated that they are also directional-selective with respect to their  $Ca^{2+}$  response, highlighting that there are other signals, timescales, and ions that important for the input selectivity.

The role of  $Ca^{2+}$  in neural signalling has been investigated experimentally and theoretically, for its involvement in shaping neural responses, uses as a selective marker/secondary messenger, and its involvement during learning and memory. To obtain a better understanding of the impact of  $Ca^{2+}$  dynamics on these neural processes and the role of propagating calcium waves in dendrites (Coombes, 2001; Keizer et al., 1998; Thul et al., 2008) and the generation of direction-selective responses in SAC (Bootman et al., 2012; Koizumi & Poznanski, 2015).

Influx of  $Ca^{2+}$  into the cytosol of neuronal dendrites, including those of SACs, occurs through calcium-dependent ion channels in the membrane, like the L-Type calcium channel, and by the calcium-induced activation of ryanodine receptor (RyRs) in the ER, which leads to the efflux of  $Ca^{2+}$  from the ER to the cytosol. This process of CICR will consequently induces more RyRs to open more  $Ca^{2+}$  channels in the membrane of the dendrite. This leads to a near continuous release of  $Ca^{2+}$  resulting in an increase the  $Ca^{2+}$  concentration level until it becomes too high, leading to

the activation of  $Ca^{2+}$  pumps to remove  $Ca^{2+}$  from the cytosol back into the ER or extruded out of the cell. This underlying mechanism for CICR leads to  $Ca^{2+}$  wave propagation in neuronal dendrites while subject to a  $Ca^{2+}$  buffer. In order to support this calcium wave along the dendrite, the timing between CICR events require to be precisely timed or else the wave will fail to propagate. To analyse this mechanism and the underlying dynamics resulting from CICR, a mathematical model of  $Ca^{2+}$  dynamics is presented that is subject to the effects of a  $Ca^{2+}$  buffer. This model is analysed with a focus on the conditions for supporting the resultant travelling  $Ca^{2+}$  wave in the presence of a buffer.

# 2. Methods

This paper presents a mathematical model for a two-pool CICR mechanism, and solves it using advanced Green's function techniques. This is the crucial step before progressing to the next step, which is the simulation. In the first step, the construction of an algorithm and mathematical model for the CICR mechanism will employ a mix of numerical and analytical approaches. First, we adopt a simple model that captures the nature of the CICR mechanism, yet is amenable to analytical techniques, before progressing to the next step, which is the analysis of underlying the support of a calcium wave in the presence of an unsaturated buffer.

# 2.1. The two-pool model equations for CICR

We consider a section of dendrite to be a cable of finite length ( $\ell$ ) and extend the CICR two-pool model of Kuba & Takeshita (1981) and Goldbeter & Berridge (1990) to involve spatial effects of  $Ca^{2+}$  signalling via diffusion. We assume a model of calcium induced calcium release (CICR) where upon increases in  $[Ca^{2+}]_i$  then so does the likelihood of release of free  $Ca^{2+}$  from the ER, and therefore  $Ca^{2+}$  stimulates its own release. Fig. 1 illustrates a schematic of the two-pool model of the CICR mechanism incorporating spatial aspects of  $Ca^{2+}$  signalling along a section of dendrite, which includes as a calcium buffer dynamics and  $Ca^{2+}$  release from the ER via RyR receptor activation. The (extended) model sets out to explore spatial aspects of Ca<sup>2+</sup> signalling along a cable representing a neuronal dendrite in the presence of a buffer.

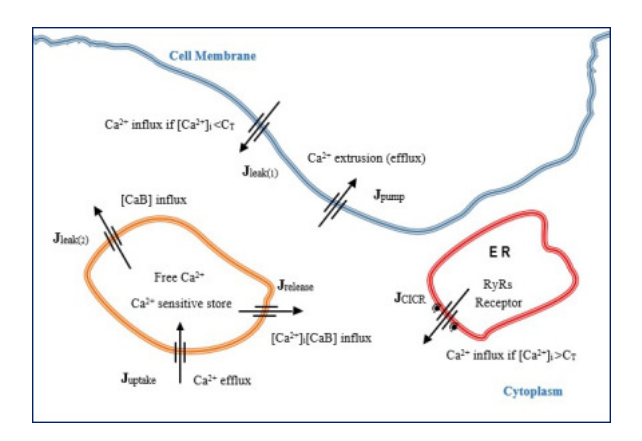


**Figure 1:** CICR mechanism operation in a two-pool model of a section of the dendritic cytoplasm.

Formally, Fig.1 describes important processes and dynamics used to describe the two pool model of CICR, where  $[Ca^{2+}]_i$  represents the free intracellular calcium concentration; [CaB] is the concentration of bound buffer to  $Ca^{2+}$ ; RyR are the Ryanodine receptors which are essentially calcium-gated ion channels located along the ER that take part in releasing  $Ca^{2+}$  into the cytoplasm of the dendrite;  $J_{\text{pump}}$  denotes  $Ca^{2+}$ pump responsible for calcium efflux out of the cytoplasm via a molecular energy based process involving Adenosine Triphosphate (ATP); ICICR represents the calcium puffs/sparks released into the cytoplasm through the activation of RyRs along the ER when  $[Ca^{2+}]_i > C_T$  where  $C_T$  is some threshold  $Ca^{2+}$  level for calcium puffs to occur;  $J_{\text{uptake}}$  denotes  $Ca^{2+}$  efflux from cytoplasm into the  $Ca^{2+}$  sensitive pool;  $J_{\text{release}}$  is influx of free  $Ca^{2+}$  and  $Ca^{2+}$  bound to the buffer from the  $Ca^{2+}$ sensitive pool into the cytoplasm;  $I_{leak}(1)$  is  $Ca^{2+}$ influx into the cytoplasm through  $Ca^{2+}$ -dependent ionic channels;  $J_{leak(2)}$  is influx of  $Ca^{2+}$  bound from the  $Ca^{2+}$  sensitive pool into the cytoplasm.

From **Fig. 1**, there are two pools inside the cytoplasm. The first pool (orange circle) represents the calcium buffer and the second (red circle) is the pool representing the endoplasmic reticulum (ER). As the dendrites intracellular  $[(Ca^{2+}]_i]_i$  increases, so does release of free  $Ca^{2+}$  from the ER, a nonlinear calcium-dependent process where  $Ca^{2+}$  induces its own further release; this autocatalytic amplification is called calcium-induced calcium release (CICR).

By taking into consideration the processes presented in **Fig. 1**, we begin to formulate our model system by considering the release of  $Ca^{2+}$  from intracellular sources, in particular the ER via CICR mechanism. The dynamics involve interactions with an internal buffer and  $Ca^{2+}$  extrusion processes. The starting point of the model is to allow one to investigate dynamic changes to  $Ca^{2+}$ -dependent excitability, the spatial diffusion dynamics of  $Ca^{2+}$ -signalling, and the impact of a buffer on  $Ca^{2+}$  spatial dynamics. For simplicity, we will assume the diffusion of both calcium and a single buffer species where Fick's law applies to a 1D cable structure where the dynamics of  $Ca^{2+}$  diffusion is given by

$$\frac{\partial [Ca^{2+}]_i}{\partial t} = D_{\text{Ca}} \frac{\partial^2 [Ca^{2+}]_i}{\partial x^2} - \text{Buffer} + J_{\text{leak}}$$
$$-P([Ca^{2+}]_i) + \sum_{j=1}^N v_{\text{CICR}}^j H([Ca^{2+}]_i - C_T) \delta(x - x_j)$$

where x is the physical position along the cable of (cm), t is the time in (sec),  $D_{Ca}$  is the diffusion constant of free calcium ( $\mu m^2/sec$ ), "Buffer" represents the calcium buffer,  $J_{leak}$  is the leak  $Ca^{2+}$  influx,  $P([Ca^{2+}]_i)$  represents a calcium pump that describes the removal of calcium ions (in order to maintain  $Ca^{2+}$  homeostasis) through an ATP-driven  $Ca^{2+}$  extrusion system,  $\nu_{CICR}$  denotes the calcium current density through RyR channels ( $\mu$ M/sec), H is the Heaviside step-function,  $C_T$ is the RyR activation threshold ( $\mu$ M) required to generate a calcium puff/spark, and  $\delta$  is the Dirac delta function (whose dimensions are the inverse of its argument). The final term describes the  $Ca^{2+}$ -dependent activation of RyR in the ER which lead to an increase in cytosolic calcium via CICR release from the ER, when the calcium concentration exceeds a threshold  $C_T$ . Note that this process is nonlinear where the shape of the  $Ca^{2+}$  input in time describes by what is called a spark/puff, whose duration can vary depending on the local dynamics of  $Ca^{2+}$ , individually modelled as square pulse whose time duration can vary between release events in a Ca<sup>2+</sup>-dependent manner.

For the buffer, the rate which it binds to calcium is proportional to the  $[Ca^{2+}]_i$  and the free buffer concentrations. The buffer also dissociates from  $Ca^{2+}$  at a rate proportional to the concentration of

the complex. This allows one to write down the corresponding buffer dynamics as:

$$\begin{split} \frac{\partial [CaM]}{\partial t} &= D_{\text{CaM}} \frac{\partial^2 [CaM]}{\partial x^2} - b[CaM] \\ &+ f \Big( [B]_{\text{TOTAL}} - [CaM] \Big) [Ca^{2+}]_i, \end{split}$$

where f and b are the forward and backward reaction rates with units  $\mu M^{-1}$  msec<sup>-1</sup> and msec<sup>-1</sup>, respectively,  $D_{\text{CaM}}$  is the diffusion constant for the calcium bound buffer with units  $\mu m^2/\text{sec}$ , and  $[B]_{\text{TOTAL}} = [CaM] + [M]$  is the total concentration of calcium bound [CaM] and unbound [M] buffer, respectively.

The extrusion of calcium occurs through high affinity and low capacity ATP-operated  $Ca^{2+}$  pumps, which are assumed to be homogeneously distributed over the dendritic membrane, and whose dynamics follows the following Hill-type expression:

$$P([Ca^{2+}]_i) = \frac{4P_{\rm m}}{d} K_{\rm P} \frac{[Ca^{2+}]_i}{[Ca^{2+}]_i + K_{\rm P}}'$$

where  $P_{\rm m}$  is the membrane pump parameter (m/sec),  $K_{\rm P}$  ( $\mu$ M) is the pump dissociation constant and the 4/d is the area-to-volume ratio for a cable of diameter d (cm). Now assuming  $Ca^{2+}$  concentration is much lower than the pump dissociation constant  $K_{\rm P}$ , this is a reasonable approximation. If a high mobile buffer concentration is present, permitting these homogeneously distributed pumps over the dendrite membrane to extrude endogenous  $Ca^{2+}$  in a linear manner. This linear behaviour can be deduced and follows the following Hill-type expression:

$$\lim_{[Ca^{2+}]_i << K_{\rm P}} P([Ca^{2+}]_i) \to \gamma [Ca^{2+}]_i.$$

This has become known as the excess buffer approximation (EBA), where the assumption of unsaturability of the  $Ca^{2+}$  buffer is likely to be valid for low  $Ca^{2+}$  concentrations or when there is an excess of available buffer.

Under these conditions, the spatiotemporal dynamics of calcium diffusion within dendrites can be

rewritten as

$$\frac{\partial [Ca^{2+}]_i}{\partial t} = D_{\text{Ca}} \frac{\partial^2 [Ca^{2+}]_i}{\partial x^2} - (\gamma + f[B]_{\text{TOTAL}}) [Ca^{2+}]_i 
+ \frac{f[B]_{\text{TOTAL}}}{k_0} [CaM] 
+ \sum_{j=1}^N v_{\text{CICR}}^j H([Ca^{2+}]_i - C_T) \delta(x - x_j) 
\frac{\partial [CaM]}{\partial t} = D_{\text{CaM}} \frac{\partial^2 [CaM]}{\partial x^2} - \frac{f[B]_{\text{TOTAL}}}{k_0} [CaM] 
+ f[B]_{\text{TOTAL}} [Ca^{2+}]_i.$$
(1)

A solution to the above reaction-diffusion system can be expressed as an integral equation involving the Green's function:

$$[Ca^{2+}]_i(x,t) = \int_0^L \int_0^t \sum_{j=1}^N v_{CICR}^j G_{Ca}(x,\zeta,t-s)$$
$$\times H([Ca^{2+}]_i(\zeta,s) - C_T) \delta(\zeta - x_j) ds d\zeta,$$

where integrating over the spatial variable  $\zeta$  leads to the following integral equation:

$$[Ca^{2+}]_{i}(x,t) = \sum_{j=1}^{N} v_{CICR}^{j} \int_{0}^{t} G_{Ca}(x,x_{j},t-s) \times H([Ca^{2+}]_{i}(x_{j},s) - C_{T}) ds$$
 (2)

The Green's function satisfies the following system of reaction-diffusion equations,

$$\frac{\partial [Ca^{2+}]_i}{\partial t} = D_{\text{Ca}} \frac{\partial^2 [Ca^{2+}]_i}{\partial x^2} - (\gamma + f[B]_{\text{TOTAL}}) [Ca^{2+}]_i \\
+ \frac{f[B]_{\text{TOTAL}}}{k_0} [CaM] \\
\frac{\partial [CaM]}{\partial t} = D_{\text{CaM}} \frac{\partial^2 [CaM]}{\partial x^2} - \frac{f[B]_{\text{TOTAL}}}{k_0} [CaM] \\
+ f[B]_{\text{TOTAL}} [Ca^{2+}]_i. \tag{3}$$

The Green's function for our coupled system of reaction-diffusion Eqn (3) are difficult to find, but can be obtained via the formal solutions presented in Hill (1981). These formal solutions have been obtained by uncoupling the system Eqn (3) using an affine mapping technique that involves a Green's function solution to a nonlinear integro-partial differential equation of the Riccati type (see section 4, pages 132-157, Lions

(1971)). Hill presented a general procedure to obtain closed form representations to the solutions of a coupled linear reaction-diffusion system including the corresponding boundary conditions. The coupled system is formally reduced to two boundary value problems involving the classical heat equation, whose solutions are given in terms of integrals involving the Green's function of the heat equation. Note that Hill (1981) illustrated that this method can also be applied to systems of non-homogeneous reaction-diffusion systems.

The formal solutions for the Green's functions for the system of reaction-diffusion equations given by Eqn (3) are

$$G_{Ca}(x, x_{j}, t) = e^{-at} \mathcal{G}_{Ca}(x, x_{j}, D_{Ca}t)$$

$$+ \frac{e^{\lambda t}}{D_{Ca} - D_{CaM}} \int_{D_{CaM}}^{D_{Ca}t} e^{-\mu \xi}$$

$$\times \left\{ \sqrt{bc} \left( \frac{\xi - D_{CaM}t}{D_{Ca}t - \xi} \right)^{\frac{1}{2}} I_{1}(\eta) \mathcal{G}_{Ca}(x, x_{j}, \xi) + bI_{0}(\eta) \mathcal{G}_{CaM}(x, x_{j}, \xi) \right\} d\xi,$$

$$(4)$$

$$G_{CaM}(x, x_{j}, t) = e^{-dt} \mathcal{G}_{CaM}(x, x_{j}, D_{CaM}t)$$

$$+ \frac{e^{\lambda t}}{D_{Ca} - D_{CaM}} \int_{D_{CaM}t}^{D_{Ca}t} e^{-\mu \xi}$$

$$\times \left\{ \sqrt{bc} \left( \frac{D_{Ca}t - \xi}{\xi - D_{CaM}t} \right)^{\frac{1}{2}} I_{1}(\eta) \mathcal{G}_{CaM}(x, x_{j}, \xi) + cI_{0}(\eta) \mathcal{G}_{Ca}(x, x_{j}, \xi) \right\} d\xi,$$

$$(5)$$

where the constants are given by

$$a = (\gamma + f[B]_{\text{TOTAL}}), \quad b = \frac{f[B]_{\text{TOTAL}}}{k_0}$$

$$c = f[B]_{\text{TOTAL}}, \quad d = \frac{f[B]_{\text{TOTAL}}}{k_0}$$

$$\lambda = \left(\frac{aD_{\text{CaM}} - dD_{\text{Ca}}}{D_{\text{Ca}} - D_{\text{CaM}}}\right), \quad \mu = \left(\frac{a - d}{D_{\text{Ca}} - D_{\text{CaM}}}\right),$$

$$\eta = \frac{2\sqrt{bc}}{D_{\text{Ca}} - D_{\text{CaM}}} \left[ (D_{\text{Ca}}t - \xi)(\xi - D_{\text{CaM}}t) \right]^{\frac{1}{2}},$$

and  $I_0$  and  $I_1$  are the modified Bessel functions. Note the  $\mathcal{G}_{Ca}$  and  $\mathscr{G}_{CaM}$  are the Green's function solutions to their corresponding heat equations

$$\frac{\partial \mathcal{G}_{Ca}}{\partial t} \left( x, x_{j}, t \right) = \frac{\partial^{2} \mathcal{G}_{Ca}}{\partial x^{2}} \left( x, x_{j}, t \right) \tag{6}$$

and

$$\frac{\partial \mathcal{G}_{CaM}}{\partial t}(x, x_1, t) = \frac{\partial^2 \mathcal{G}_{CaM}}{\partial x^2}(x, x_1, t).$$
 (7)

One can calculate the corresponding solutions for Eqns (6) and (7) via Laplace transform techniques to arrive at the following expressions for  $\mathcal{G}_{Ca}$  and  $\mathcal{G}_{CaM}$  (see Appendix).

Having determined  $G_{Ca}(x, x_j, t)$  and  $G_{CaM}(x, x_l, t)$ , one can now focus on developing an efficient solution for the formal solutions of  $G_{Ca}(x, x_j, t)$  and  $G_{CaM}(x, x_l, t)$ , respectively. Closer inspection of the formal solutions given by Eqns (4) & (5), one notices that it involves a mathematical form with some similarity to a convolution integral. This can be better seen by applying the following transformation of variables,

$$\xi = D_{\text{CaM}}t + (D_{\text{Ca}} - D_{\text{CaM}})\tau$$

This allows Eqns (4) and (5) to be rewritten as

$$G_{Ca}(x, x_{j}, t) = e^{-at} \mathcal{G}_{Ca}(x, x_{j}, D_{Ca}t)$$

$$+ e^{(\lambda - \mu b_{1})t} \int_{0}^{t} e^{-\mu b_{2}\tau}$$

$$\times \left\{ \sqrt{bc} \left( \frac{\tau}{t - \tau} \right)^{\frac{1}{2}} I_{1}(\eta) \mathcal{G}_{Ca}(x, x_{j}, b_{1}t + b_{2}\tau) + bI_{0}(\eta) \mathcal{G}_{CaM}(x, x_{j}, b_{1}t + b_{2}\tau) \right\} d\tau,$$
(8)

$$G_{CaM}(x, x_{j}, t) = e^{-dt} \mathcal{G}_{CaM}(x, x_{j}, D_{CaM}t)$$

$$+ e^{(\lambda - \mu b_{1}t)} \int_{0}^{t} e^{-\mu b_{2}\tau} dt$$

$$\times \left\{ \sqrt{bc} \left( \frac{t - \tau}{\tau} \right)^{\frac{1}{2}} I_{1}(\eta) \mathcal{G}_{CaM}(x, x_{j}, b_{1}t + b_{2}\tau) + cI_{0}(\eta) \mathcal{G}_{Ca}(x, x_{j}, b_{1}t + b_{2}\tau) \right\} d\tau,$$

$$(9)$$

where 
$$b_1 = D_{\text{CaM}}$$
,  $b_2 = D_{\text{Ca}} - D_{\text{CaM}}$ , and  $\eta = 2\sqrt{bc}[\tau(t-\tau)]^{\frac{1}{2}}$ 

Observation of Eqns (8) and (9) highlights that the integral parts represent a generalized convolution

and show some similarity to the traditional convolution integral and to some extent are also dependent on non-euclidean/deformed warping involving two time variables. Furthermore, the reader should not that the argument appearing in the modified Bessel functions strictly does not a resemble convolution, but a higher-order nonlinear temporal dependence. Unfortunately, there are no closed-form solutions to the aforementioned equations thus these integrals need to be calculated numerically. Given this fact, there is a potential approximation which can be employed that may permit a obtaining a closed-form expression for the corresponding approximation. Note that in both Eqns (8) and (9) one can perform a Taylor expansion of the corresponding Green's functions  $\mathscr{G}_{CaM}(x, x_i, b_1 t + b_2 \tau)$  and  $\mathscr{G}_{CaM}(x, x_i, b_1 t + b_2 \tau)$ . This leads to the integral component of Eqn (8) to be expressed as,

$$\int_{0}^{t} e^{-\mu b_{2}\tau} \times \left\{ \sqrt{bc} \left( \frac{\tau}{t-\tau} \right)^{\frac{1}{2}} I_{1}(\eta) \times \right.$$

$$\left. \sum_{n=0}^{\infty} \frac{(b_{1}t)^{n}}{n!} \frac{\partial^{n} \mathcal{G}_{Ca}}{\partial \tau^{n}}(x, x_{j}, b_{2}\tau) + bI_{0}(\eta) \sum_{n=0}^{\infty} \frac{(b_{1}t)^{n}}{n!} \frac{\partial^{n} \mathcal{G}_{CaM}}{\partial \tau^{n}}(x, x_{j}, b_{2}\tau) \right\} d\tau,$$

noting that the expression for the integral component of Eqn (9) takes the following similar form

$$\int_{0}^{t} e^{-\mu b_{2}\tau} \times \left\{ \sqrt{bc} \left( \frac{t-\tau}{\tau} \right)^{\frac{1}{2}} I_{1}(\eta) \times \right.$$

$$\left. \sum_{n=0}^{\infty} \frac{(b_{1}t)^{n}}{n!} \frac{\partial^{n} \mathcal{G}_{\text{CaM}}}{\partial \tau^{n}} (x, x_{j}, b_{2}\tau) + bI_{0}(\eta) \sum_{n=0}^{\infty} \frac{(b_{1}t)^{n}}{n!} \frac{\partial^{n} \mathcal{G}_{\text{Ca}}}{\partial \tau^{n}} (x, x_{j}, b_{2}\tau) \right\} d\tau,$$

Now keeping the first terms in both Eqns (8) and (9).

$$\begin{split} \int_0^t e^{-\mu b_2 \tau} \\ & \times \bigg\{ \sqrt{bc} \left( \frac{\tau}{t-\tau} \right)^{\frac{1}{2}} I_1(\eta) \mathcal{G}_{\mathsf{Ca}}(x,x_{\mathsf{j}},b_2 \tau) \\ & + b I_0(\eta) \mathcal{G}_{\mathsf{CaM}}(x,x_{\mathsf{j}},b_2 \tau) \bigg\} d\tau, \end{split}$$

and

$$\begin{split} \int_0^t e^{-\mu b_2 \tau} \\ \bigg\{ \sqrt{bc} \left( \frac{t-\tau}{\tau} \right)^{\frac{1}{2}} I_1(\eta) \mathcal{G}_{\mathsf{CaM}}(x,x_{\mathsf{j}},b_2 \tau) \\ &+ b I_0(\eta) \mathcal{G}_{\mathsf{Ca}}(x,x_{\mathsf{j}},b_2 \tau) \bigg\} d\tau. \end{split}$$

then from this truncated series, a closed-form expression could be obtained for  $G_{\text{CaM}}(x, x_j, t)$  by using the following identity,

$$\mathcal{L}\left[\int_0^t \left(\frac{t-\tau}{\tau}\right)^{\frac{\nu}{2}} I_{\nu}\left(a\sqrt{\tau(t-\tau)}\right) f(\tau) d\tau\right] =$$

$$= \left(\frac{a}{2}\right)^{\nu} s^{-(\nu+1)} F\left(s - \frac{a^2}{4s}\right),$$

where  $f(\tau) = e^{-\mu(D_{Ca}-D_{CaM})\tau}\mathcal{G}_{CaM}(x, x_j, b_2\tau)$  or  $f(\tau) = e^{-\mu(D_{Ca}-D_{CaM})\tau}\mathcal{G}_{Ca}(x, x_j, b_2\tau)$  where appropriate, however a closed form expression for the truncated series for  $G_{Ca}(x_i, x_j, t)$ 

$$\int_0^t \left(\frac{t-\tau}{\tau}\right)^{\frac{\nu}{2}} I_{\nu}\left(a\sqrt{\tau(t-\tau)}\right) f(\tau) d\tau$$

could be calculated analytically, involving a series representation of the  $I_{\nu}$  resulting in an infinite series that may not be represented by a closed-form expression, and thus leads to serious concerns about computation and accuracy. In this case it is preferable to apply numerical techniques to calculate the generalized integral directly.

#### 3. Results

In order to proceed, the resulting Green's functions,  $\mathcal{G}_{Ca}(x, x_j, t)$  and  $\mathcal{G}_{CaM}(x, x_l, t)$  are calculated using MATLAB's inbuilt integral function. In **Fig.** 2, some examples of these Green's functions are presented at various locations, keeping in mind that these represent the zeroth order for the calcium  $[Ca^{2+}]_i$  and buffer [CaM] concentrations, respectively.

# 3.1. Support for saltatory calcium waves

To explore the properties of saltatory waves and the conditions that support this, one needs to observe how the spacing between RyR and their respective activation times impacts wave propagation. Here, our calcium system presented in Eqn (1) describes the evolution of calcium through the assumption that  $[Ca^{2+}]_i$  is continuously removed while being

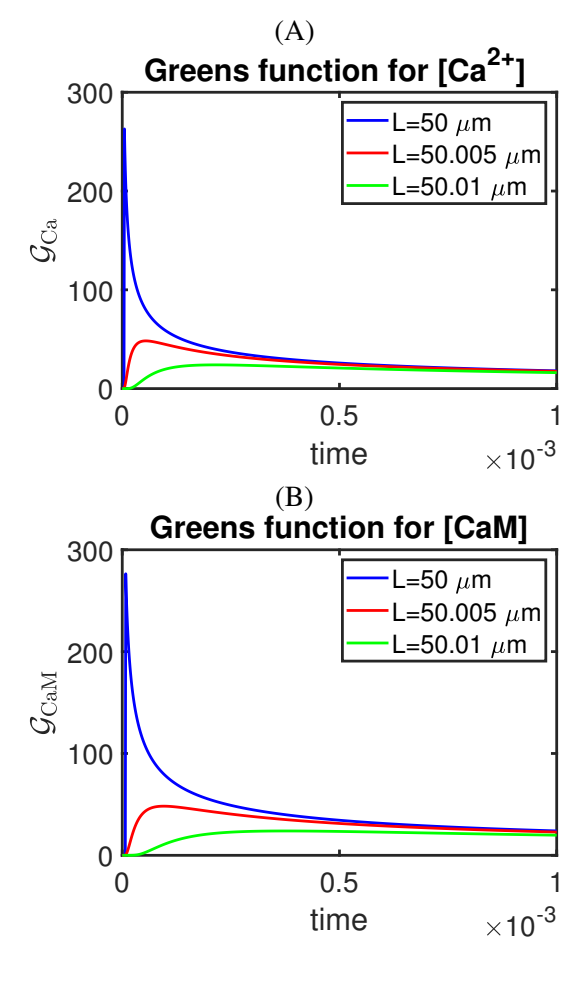


**Figure 2:** Example plots of the Green's function associated with (A) calcium  $\mathcal{G}_{Ca}(x,x_j,t)$  and the (B) calcium buffer  $\mathcal{G}_{CaM}(x,x_j,t)$  taken at three different distances from a specific source location  $x_i = 0.5\ell$ 

released from discrete sites where the RyR in the presence of a buffer. Noting that calcium release from the RyRs are calcium dependent and occurs when  $[Ca^{2+}]_i$  reaches some threshold value  $C_T$  at some release site and instantaneously releases a discrete amount of  $[Ca^{2+}]$  into the cytosol of the dendrite. This mechanism permits the propagation of a  $[Ca^{2+}]$  wave through the sequential puffs coming from the firing of RyR release sites, each responding to  $[Ca^{2+}]$  diffusing from nearby RyR release sites, along the direction of the travelling wave, that can support saltatory propagation and hence the timing of these events is important for its propagation, resembling a *fire-diffuse-fire* process.

Noting that the integral equation, represented by Eqn (2), describes  $[Ca^{2+}]$  evolution through the action of the system's Green's function and the discrete, yet  $[Ca^{2+}]$ -dependent CICR via the RyRs at

specific times  $t_j$ . One can apply a useful approximation to Eqn (2) by assuming these puff release events can be modelled by delta functions, Eqn (2) can be expressed as

$$[Ca^{2+}]_i(x,t) = \int_0^t \sum_{j=1}^N v_{CICR}^j G_{Ca}(x,x_j,t-s) \times H([Ca^{2+}]_i(x_j,s) - C_T) \delta(s-t_j) ds,$$

Now lets consider that the location of RyR are equally spaced along the ER with a distance between these release sites of  $\Delta x$ , thus

$$[Ca^{2+}]_i(x,t) = \sum_{j=1}^N v_{CICR}^j G_{Ca}(x,x_j,t-t_j) \times H([Ca^{2+}]_i(x_j,t_j) - C_T).$$

Here,  $t_j$  is the time where  $[Ca^{2+}]$  at position  $x_j$  first reaches the threshold value of  $C_T$  at the  $j^{th}$  RyR release site. When this occurs, the  $j^{th}$  site releases a calcium puff of size  $v_{CICR}^j$ , where the dependence of the  $j^{th}$  depends on the evolution of  $[Ca^{2+}]$  concentration, and for a single puff from site j the calcium profile is given by the Green's function  $\mathcal{G}_{Ca}(x,x_j,t)$ ,

$$[Ca^{2+}]_i^j(x,t) = v_{CICR}^j G_{Ca}(x,x_j,t-t_j)H(t-t_j),$$

where H is the Heaviside step function and noting that  $G_{Ca}(x, x_j, t - t_j)H(t - t_j)$  is the solution to our reaction-diffusion system for an impulse input at  $x = x_j$  at  $t = t_j$  (Hill, 1981). Superimposing the contribution from each site, we arrive at

$$[Ca^{2+}]_i(x,t) = \sum_{j=1}^N v_{\text{CICR}}^j G_{\text{Ca}}(x,x_j,t-t_j) H(t-t_j),$$

noting that calcium concentration  $[Ca^{2+}]_i$  is not a continuous function of time t at any release site  $x_j$ . Let's consider that the amount of  $[Ca^{2+}]$  released at sites  $j = M, M - 1, \ldots$  was identical and small, namely  $v_{\text{CICR}}^j = v_{\text{CICR}}$  and whose activation times were known and consistent  $t_M > t_{M-1} > \ldots$  Now the next release event at time  $t_{M+1}$  at  $t_{M+1}$  occurs when  $[Ca^{2+}]_i$  at  $t_{M+1}$  first reaches threshold  $t_{M+1}$  that is,

$$\begin{split} &[Ca^{2+}]_i((M+1)\Delta x,t_{M+1}^-) = C_{\rm T},\\ &\frac{\partial}{\partial t}[Ca^{2+}]_i((M+1)\Delta x,t_{M+1}^-) > 0. \end{split}$$

Now,  $t_{M+1}$  must satisfies

$$C_{\rm T} = \sum_{j \le M} \nu_{\rm CICR} G_{\rm Ca}(x_{\rm M+1}, x_{\rm M}, t_{\rm M+1} - t_{\rm M}).$$

Now for a wave to propagate corresponds to the situation of having  $t_j - t_{j-1} = \tau$ , where  $\tau$  is a constant for all release sites j, that is, each site releases a  $[Ca^{2+}]$  puff at a fixed time after the preceding release site had released a puff. Therefore a propagating solution exist when  $t_{M+1}-t_j = \tau(M+1-j)$ , and  $\tau$  is a solution to the following equation satisfying,

$$\begin{split} \frac{C_{\mathrm{T}}}{\nu_{\mathrm{CICR}}} &= \sum_{j \leq M} G_{\mathrm{Ca}}((M+1)\Delta x, j\Delta x, \tau(M+1-j)), \\ &\equiv \sum_{m=1}^{N} \overline{G}_{\mathrm{Ca}}(\Delta x, m, \tau) \equiv \overline{\mathcal{G}}(m, \Delta x, \tau, N), \end{split}$$

where  $\overline{G}_{Ca}(\Delta x, m, \tau)$  is given by

$$\begin{split} \overline{G}_{\text{Ca}}(\Delta x, m, \tau) &= \\ e^{-a\tau m} \mathcal{G}_{\text{Ca}}((M+1)\Delta x, j\Delta x, D_{\text{Ca}}\tau m) \\ &+ e^{(\lambda - \mu b_1)\tau m} \int_0^{\tau m} e^{-\mu b_2 \rho} \\ &\times \bigg\{ \sqrt{bc} \bigg( \frac{\rho}{\tau m - \rho} \bigg)^{\frac{1}{2}} I_1(\eta) \\ &\quad \times \mathcal{G}_{\text{Ca}}((M+1)\Delta x, j\Delta x, b_1 \tau m + b_2 \rho) \\ &+ b I_0(\eta) \mathcal{G}_{\text{CaM}}((M+1)\Delta x, j\Delta x, b_1 t\tau m + b_2 \rho) \bigg\} d\rho, \end{split}$$

$$\begin{split} \overline{G}_{\text{Ca}}(\Delta x, m, \tau) &= \\ e^{-a\tau m} \mathcal{G}^{\star}_{\text{Ca}}(m\Delta x, D_{\text{Ca}}\tau m) \\ &+ e^{(\lambda - \mu b_{1})\tau m} \int_{0}^{\tau m} e^{-\mu b_{2}\rho} \\ &\times \left\{ \sqrt{bc} \left( \frac{\rho}{\tau m - \rho} \right)^{\frac{1}{2}} I_{1}(\eta) \right. \\ &\times \mathcal{G}^{\star}_{\text{Ca}}(m\Delta x, b_{1}\tau m + b_{2}\rho) \\ &+ bI_{0}(\eta) \mathcal{G}^{\star}_{\text{CaM}}(m\Delta x, b_{1}\tau m + b_{2}\rho) \right\} d\rho, \end{split}$$

$$\text{where } \eta = 2\sqrt{bc} [\rho(\tau m - \rho)]^{1/2}, m = (M+1) - j$$

$$\mathcal{G}_{\text{Ca}}((M+1)\Delta x, j\Delta x, b_{1}\tau m + b_{2}\rho) \\ &= \mathcal{G}^{\star}_{\text{Ca}}((M+1) - j)\Delta x, b_{1}\tau m + b_{2}\rho) \\ &= \mathcal{G}^{\star}_{\text{Ca}}(m\Delta x, b_{1}\tau m + b_{2}\rho), \end{split}$$

where  $\mathcal{G}^{\star}_{Ca}(m\Delta x, b_1\tau m + b_2\rho)$  is expressed in terms of the form

$$\mathcal{G}^{\star}_{Ca}(m\Delta x, \tau m)$$

$$= \frac{1}{\sqrt{4\pi\tau m}} \left[ e^{(m-2nN)^2 \Delta x^2/(4\tau m)} + \text{similar terms} \right]$$

**Fig. 2** is a plot of  $\overline{\mathcal{G}}(m, \Delta x, \tau, N)$ , where we have used the parameters listed in Table 1 (see Appendix).

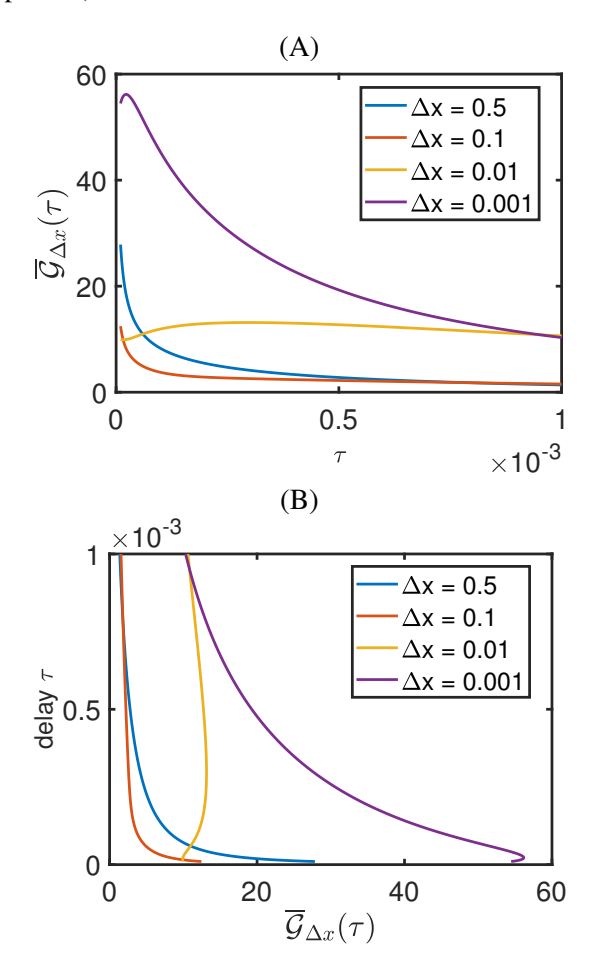


**Figure 3:** Plots of (A)  $\overline{\mathcal{G}}_{\Delta x}(\tau)$  and the delay (B)  $\tau$  for several values of  $\Delta x$ . Note that some of profiles in (A) are monotonically decreasing but the others have maximal values.

The plots of **Fig. 3A** are presented for several values of  $\Delta x$ , in particular, for some values of  $\Delta x$ , the function  $\overline{\mathcal{G}}_{\Delta x}(\tau)$  is not monotone increasing, but has a maximal  $\overline{\mathcal{G}}_{\Delta x}$  value, say  $\overline{\mathcal{G}}_{\max}(\Delta x)$ , which is a concave function of  $\Delta x$  (data not shown). Note that,  $\overline{\mathcal{G}}_{\Delta x}(\tau) \to \beta$ , where  $\beta$  has some finite value as  $\tau \to 0$ , but  $\overline{\mathcal{G}}_{\Delta x}(\tau) \to 0$  as  $\tau \to \infty$ . Now for the condition that  $C_T/\nu_{\text{CICR}} > \overline{\mathcal{G}}_{\max}(\Delta x)$  then propagation failure

is expected, but if  $C_{\rm T}/\nu_{\rm CICR} < \overline{\mathcal{G}}_{\rm max}(\Delta x)$ , then a physical solution is expected, corresponding to the time when  $[Ca^{2+}]$  first crosses the threshold  $C_{\rm T}$ .

For larger values of  $\tau$ , the function  $\overline{\mathcal{G}}_{max}(\Delta x)$  has a concave profile (data not shown) and potentially agrees with the function  $\exp(-\Delta x)$ . This gives us an approximate criterion for propagation failure, that is when  $C_T/\nu_{CICR} > \exp(-\Delta x)$ , the saltatory wave fails to propagate, but keeping in mind that both calcium and buffer diffusion constants influence this criterion.

For **Fig.** (3B), we have plotted the delay  $\tau$  as a function of  $C_T/\nu_{CICR}$  ( $\overline{\mathcal{G}}_{\Delta x}(\tau)$ ) by reversing the axes in **Fig. 3A**. Note that with  $\tau \neq 0$  one expects the propagation of the wave to fail at some positive velocity. Thus, when the distance between release sites, or the threshold is too large, or the amount of  $\nu_{CICR}$  calcium released is not sufficient, then propagation fails.

In **Fig. 4**, we have plotted the buffer function  $\overline{\mathcal{H}}_{\Delta x}(\tau)$  and its corresponding delay  $\tau$  in a similar manner as  $\overline{\mathcal{G}}_{\Delta x}(\tau)$  using the constants presented in Table1 (see Appendix). Here, in **Fig. 4A** presents curves that monotonically increasing, where each tend towards to some maximum or finite asymptotic value. The plots from **Fig. 3-4**, are also indicating the potential for saltatory buffer waves could be present while calcium waves have failed.

# 4. Discussion

Analytical solutions of reaction-diffusion systems have not attracted as much attention due to the difficulty in solving such systems, especially when there are nonlinearities present; in favour of numerical approaches based on sacrificing continuity with a chain of discrete isopotential compartments connected to each other like a chain (D'Angelo & Jirsa, 2022; Neymotin et al., 2015). These compartments are a consequence of the discretization process applied to reactiondiffusion systems resulting in an approximation based on connected isopotential compartments, that facilitates the reaction-diffusion system to be recast into a system of ordinary differential equations, permitting numerical solutions to be calculated. Over the preceding decades, this has been the tool of choice, where biological realism is typically associated with morphologically detailed

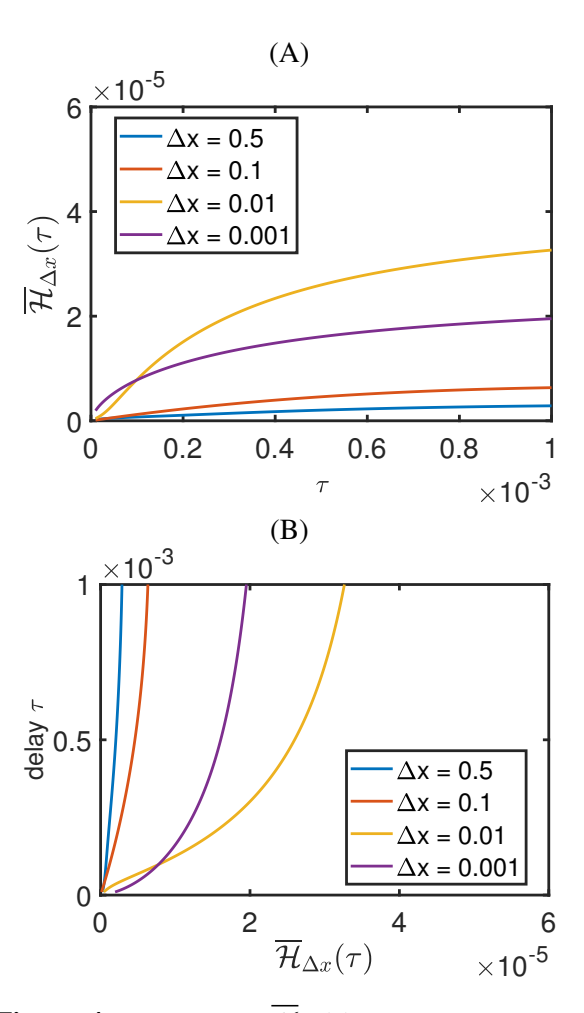


**Figure 4:** Plots of (A)  $\overline{\mathcal{H}}_{\Delta x}(\tau)$  and the delay (B)  $\tau$  for several values of  $\Delta x$ . Note that some of profiles in (A) are monotonically decreasing but the others have maximal values.

compartmental models (Bhalla, 2012; Bower & Beeman, 1998; Hines & Carnevale, 1997; Holmes & Rall, 1992; Kobayashi et al., 2021; Lindsay et al., 2007).

Here, we have returned to investigate the question of finding analytical solutions of reaction-diffusion systems and its importance for the underlying reaction-diffusion dynamics of the calcium system. Hill's solution (Hill, 1981) is a notable example to explore, although derived as a formal solution we have developed simulations using Hill's equation, but this required numerical integration to evaluate the generalized convolution appearing the Eqns (8) and (9). Unfortunately, an analytical solution was currently not possible to derive, although we have provided some interesting avenues that need to be studied. We have also taken the first steps to investigate the conditions for

supporting the propagation of saltatory waves. We adapted the method presented in Keener (2000); Keener & Sneyd (1998); Keizer et al. (1998) to use Hill's solution Hill (1981) and observed the same qualitative trends compared to these older studies where the distance between RyR release sites decreases supports the propagation of the saltatory wave.

In future, various analysis techniques, including homogenization and analysis of travelling waves need to be applied in a way that explicitly includes buffer dynamics, in order to better understand how the reaction-diffusion dynamics of calcium and buffers influence each other in general and when waves have been generated. This provides insights into the general behaviour and dynamics of such (reaction-diffusion) systems when describing the dynamics and processes involved with the introduction of proteins to the intracellular domain of dendrites and how these can be used to understand experimental procedures and the observed results, as well as how the spatiotemporal nature of these injected proteins impacts neural responses, including their influence on relevant cellular processes such as synaptic plasticity.

## **Conflicts of interest:**

The authors declare no conflict of interest.

## **Appendix**

Here, the solutions to the corresponding heat equations for both calcium and the calcium buffer are presented, where the Green's function for calcium  $\mathcal{G}_{Ca}(x,x_j,t)$  and the calcium buffer  $\mathcal{G}_{Ca}(x,x_j,t)$  are given by the solution to the following boundary value problem:

$$\begin{split} \frac{\partial \mathcal{G}_{Ca}}{\partial t} \left( x, x_{j}, t \right) &= \\ \frac{\partial^{2} \mathcal{G}_{Ca}}{\partial x^{2}} \left( x, x_{j}, t \right) + \delta \left( x - x_{j} \right) \delta \left( t - t_{i} \right) \\ \text{for } t \geq t_{i} \\ \frac{\partial \mathcal{G}_{Ca}}{\partial x} \left( 0, 0, t \right) &= \frac{\partial \mathcal{G}_{Ca}}{\partial x} (\ell, \ell, t) = 0 \\ \text{and} \\ \frac{\partial \mathcal{G}_{CaM}}{\partial t} \left( x, x_{l}, t \right) &= \\ \frac{\partial^{2} \mathcal{G}_{CaM}}{\partial x^{2}} \left( x, x_{l}, t \right) + \delta \left( x - x_{l} \right) \delta \left( t - t_{k} \right) \\ \text{for } t \geq t_{k} \end{split}$$

$$\frac{\partial \mathcal{G}_{\text{CaM}}}{\partial x}(0,0,t) = \frac{\partial \mathcal{G}_{\text{CaM}}}{\partial x}(\ell,\ell,t) = 0,$$

where the length of the cable is  $\ell$ , with sealed-end boundary conditions at both ends subject to impulse inputs at point  $x_j$  along the cable. One can solve these equations using either separation of variables (whose solution converges rapidly for large t) or Laplace transform methods whose solutions converge rapidly for all t.

There are two sort after solutions, one where there is an unit impulse at the boundary x=0 and t=0 and the other is where the impulse occurs at any position along the cable at  $x=x_j$  at time  $t=t_i$ . The solution corresponding to the response to a unit impulse at x=0 and t=0. In the case for calcium  $\mathcal{G}_{Ca}(x,0,t)$  for a finite cable with a sealedend boundary condition,  $\frac{\partial \mathcal{G}_{Ca}}{\partial x}(0,0,t)=-\delta(t)$  at x=0 and a sealed-end condition  $\frac{\partial \mathcal{G}_{Ca}}{\partial x}(\ell,0,t)=0$  at  $x=\ell$ , several representations for the Green's function converges for small t (Tuckwell, 1988) for this case, solving the case when the impulse occurs at the boundary x=0 and the above mentioned boundary value for x=0, the corresponding Green's functions  $\mathcal{G}_{Ca}(x,0,t)$  is

$$\mathcal{G}_{Ca}(x,0;t) = \frac{1}{\sqrt{4\pi t^3}} \sum_{n=0}^{\infty} (-1)^n \left\{ [2(n+1)\ell - x] \exp\left(-\frac{[2(n+1)\ell - x]^2}{4t}\right) + [2n\ell + x] \exp\left(-\frac{[2n\ell + x]^2}{4t}\right) \right\},$$

$$t > 0. \ 0 < x < \ell$$

Analogously, the corresponding Green's function for the buffer heat equation is  $\mathcal{G}_{CaM}$  is given by

$$\mathcal{G}_{CaM}(x,0;t) = \frac{1}{\sqrt{4\pi t^3}} \sum_{n=0}^{\infty} (-1)^n \left\{ [2(n+1)\ell - x] \exp\left(-\frac{[2(n+1)\ell - x]^2}{4t}\right) + [2n\ell + x] \exp\left(-\frac{[2n\ell + x]^2}{4t}\right) \right\},$$

$$t > 0. \ 0 < x < \ell.$$

Now the Green's function for unit impulses occurring along the cable  $G_{Ca}(x, x_i; t - t_i)$  is the solution

to the following,

$$\begin{split} \frac{\partial \mathcal{G}_{\text{Ca}}}{\partial t}(x, x_i; t) &= \\ \frac{\partial^2 \mathcal{G}_{\text{Ca}}}{\partial x^2}(x, x_i; t) + \delta(x - x_i)\delta(t - t_i), \quad t > t_i, \end{split}$$

with the following sealed-end boundary conditions at x = 0,  $\frac{\partial \mathcal{G}_{Ca}}{\partial x}(0, x_i; t) = 0$  and at  $x = \ell$   $\frac{\partial \mathcal{G}_{Ca}}{\partial x}(\ell, x_i, t) = 0$ . Using these initial and boundary conditions and applying both Laplace and inverse Laplace transforms, and series expansions leads to

$$\mathcal{F}_{Ca}(x, x_i; t - t_i) = \frac{1}{\sqrt{4\pi(t - t_i)}} \sum_{n=0}^{\infty} (-1)^n \left\{ \exp\left(-\frac{(x - x_i - 2n\ell)^2}{4(t - t_i)}\right) + \exp\left(-\frac{(x + x_i + 2n\ell)^2}{4(t - t_i)}\right) + \exp\left(-\frac{(x + x_i - 2(n + 1)\ell)^2}{4(t - t_i)}\right) + \exp\left(-\frac{(x - x_i + 2(n + 1)\ell)^2}{4(t - t_i)}\right) \right\}$$
for  $x < x_i$  and  $t > t_i$ 

and

$$\mathcal{H}_{Ca}(x, x_i; t - t_i) = \frac{1}{\sqrt{4\pi(t - t_i)}} \sum_{n=0}^{\infty} (-1)^n \left\{ \exp\left(-\frac{(x - x_i - 2n\ell)^2}{4(t - t_i)}\right) + \exp\left(-\frac{(x + x_i + 2n\ell)^2}{4(t - t_i)}\right) + \exp\left(-\frac{(x - x_i + 2n\ell)^2}{4(t - t_i)}\right) - \exp\left(-\frac{(x - x_i - 2n\ell)^2}{4(t - t_i)}\right), + \exp\left(-\frac{(x + x_i - 2(n + 1)\ell)^2}{4(t - t_i)}\right) + \exp\left(-\frac{(x - x_i + 2(n + 1)\ell)^2}{4(t - t_i)}\right) + \exp\left(-\frac{(x - x_i + 2(n + 1)\ell)^2}{4(t - t_i)}\right)$$

$$-\exp\left(-\frac{(x-x_i-2(n+1)\ell)^2}{4(t-t_i)}\right),$$
for  $x \ge x_i$  and  $t > t_i$ .

Combining the cases for  $x < x_i$  and  $x \ge x_i$  leads to the following Green's function,

$$\mathcal{G}_{Ca}(x, x_i; t - t_i) =$$

$$\left\{ \mathcal{F}_{Ca}(x, x_i; t - t_i) H(x_i - x) + \mathcal{H}_{Ca}(x_i, x; t - t_i) H(x - x_i) \right\} H(t - t_i),$$

$$t > t_i, \ 0 < x, x_i < \ell.$$

Similarly for the calcium buffer, the corresponding Green's function is given by

$$\mathcal{G}_{CaM}(x, x_i; t - t_i) =$$

$$\left\{ \mathcal{F}_{CaM}(x, x_i; t - t_i) H(x_i - x) + \mathcal{H}_{CaM}(x_i, x; t - t_i) H(x - x_i) \right\} H(t - t_i),$$

$$t > t_i, 0 < x, x_i < \ell.$$

where

$$\mathcal{F}_{CaM}(x, x_i; t - t_i) = \frac{1}{\sqrt{4\pi(t - t_i)}} \sum_{n=0}^{\infty} (-1)^n \left\{ \exp\left(-\frac{(x - x_i - 2n\ell)^2}{4(t - t_i)}\right) + \exp\left(-\frac{(x + x_i + 2n\ell)^2}{4(t - t_i)}\right) + \exp\left(-\frac{(x + x_i - 2(n + 1)\ell)^2}{4(t - t_i)}\right) + \exp\left(-\frac{(x - x_i + 2(n + 1)\ell)^2}{4(t - t_i)}\right) \right\}$$
for  $x < x_i$  and  $t > t_i$ 

and

$$\mathcal{H}_{CaM}(x, x_i; t - t_i) = \frac{1}{\sqrt{4\pi(t - t_i)}} \sum_{n=0}^{\infty} (-1)^n \left\{ \exp\left(-\frac{(x - x_i - 2n\ell)^2}{4(t - t_i)}\right) \right\}$$

**Table 1:** Table of constants

Notation	Description	Quantity
$[Ca^{2+}]_i$	Intracellular calcium concentration ( $\mu M$ ) where $M = mol/L$	
$[Ca^{2+}]_o$	Extracellular calcium concentration at rest $(\mu M)$	2000μΜ
t	Time (msec)	
X	Physical distance along dendrite (μm)	
$D_{Ca}$	Diffusion constant of free calcium ( $\mu m^2/msec$ )	0.23 μm²/msec
$C_{\mathrm{T}}$	Channel activation threshold ( $\mu M$ )	0.5 μΜ
$\nu_{ m CICR}$	Calcium source current density (µM/msec)	0.0027 μM/msec
$P_{\rm m}$	Pump rate (µm/msec)	0.2 μm/msec
d	Diameter of dendrite (μm)	2 μm
$[B]_{\text{TOTAL}} = [CaM] + [M]$	Total concentration of calcium binding $(\mu M)$	100 μΜ
[CaM]	Concentration of bound buffer ( $\mu M$ )	
[M]	Concentration of unbound buffer ( $\mu M$ )	
f	Forward reaction rate $(\mu Mmsec)^{-1}$	$0.320 \ (\mu M)^{-1} (msec)^{-1}$
b	Backward reaction rate (msec) <sup>-1</sup>	$0.06~(msec)^{-1}$
$K_{\rm D} = b/f$	Dissociation constant $(\mu M)$	0.20 (μM)
$D_{CaM}$	Diffusion constant of buffered calcium ( $\mu m^2/msec$ )	0.13 μm²/msec
$k_{\rm o} = [B]_{\rm TOTAL}/K_{\rm D}$	Buffer capacity (dimensionless)	500
$\gamma = \frac{4P_{\rm m}}{d}$	Constant parameter (msec) <sup>-1</sup>	0.4 (msec) <sup>-1</sup>
· · ·	Physical length along the dendrite (μm)	100 µт
$\delta[\cdot]$	Dirac delta function (inverse dimension of its argument)	
$H[\cdot]$	Heaviside step-function (dimensionless)	
$x_{i}$	Position of calcium sources (µm)	
Ń	Number of calcium RyR hotspots (dimensionless)	0-20

$$+ \exp\left(-\frac{(x+x_i+2n\ell)^2}{4(t-t_i)}\right) + \exp\left(-\frac{(x-x_i+2n\ell)^2}{4(t-t_i)}\right) - \exp\left(-\frac{(x-x_i-2n\ell)^2}{4(t-t_i)}\right), + \exp\left(-\frac{(x+x_i-2(n+1)\ell)^2}{4(t-t_i)}\right) + \exp\left(-\frac{(x-x_i+2(n+1)\ell)^2}{4(t-t_i)}\right) + \exp\left(-\frac{(x-x_i+2(n+1)\ell)^2}{4(t-t_i)}\right) - \exp\left(-\frac{(x-x_i-2(n+1)\ell)^2}{4(t-t_i)}\right),$$

for  $x \ge x_i$  and  $t > t_i$ .

#### References

Barlow, H. B., Hill, R. M. & Levick, W. R. (1964) 'Retinal ganglion cells responding selectively to direction and speed of image motion in the rabbit', *Journal of Physiology (London)* **173**, 377–407.

Barlow, H. B. & Levick, W. R. (1965) 'The mechanism of directionally selective units in rabbit's retina', *The Journal of Physiology (London)* **178**, 477–504.

Bhalla, U. S. (2012) Multi-compartmental models of neurons, *in* 'Computational Systems Neurobiology', Springer, pp. 193–225.

Blasdel, G. G. (1992) 'Orientation selectivity, preference, and continuity in monkey striate cortex', *Journal of Neuroscience* **12**(8), 3139–3161.

Bonhoeffer, T. & Grinvald, A. (1993) Optical imaging of the functional architecture in cat visual cortex: the layout of direction and orientation domains, *in* 'Optical Imaging of Brain Function and Metabolism', Springer, pp. 57–69.

Bootman, M. D., Rietdorf, K., Hardy, H., Dautova, Y., Corps, E., Pierro, C., Stapleton, E., Kang, E. & Proudfoot, D. (2012) Calcium signaling and regulation of cell function, *in* 'eLS Wiley & Sons', Chichester.

Bower, J. M. & Beeman, D. (1998) Compartmental modeling, *in* 'The Book of GENESIS: Exploring Realistic Neural Models with the GEneral NEural SImulation System', Springer, pp. 7–15.

Coombes, S. (2001) 'The effect of ion pumps on the speed of travelling waves in the fire-diffuse-fire model of Ca<sup>2+</sup> release', *Bulletin of Mathematical Biology* **63**(1), 1–20.

D'Angelo, E. & Jirsa, V. (2022) 'The quest for multiscale brain modeling', *Trends in Neurosciences* **45**, 777–790.

Euler, T., Detwiler, P. B. & Denk, W. (2002) 'Directionally selective calcium signals in dendrites of starburst amacrine cells', *Nature* **418**, 845–852.

219

Volume 4, Issue 3, 2025

- Gizzi, M. S., Katz, E., Schumer, R. A. & Movshon, J. A. (1990) 'Selectivity for orientation and direction of motion of single neurons in cat striate and extrastriate visual cortex', *Journal of Neurophysiology* **63**(6), 1529–1543.
- Goldbeter, A. D. G. & Berridge, M. J. (1990) 'Minimal model for signal-induced Ca<sup>2+</sup> oscillations and for their frequency encoding through protein phosphorylation', *Proceedings of the National Academy of Sciences* **87**(4), 1461–1465.
- Heggelund, P. & Moors, J. (1983) 'Orientation selectivity and the spatial distribution of enhancement and suppression in receptive fields of cat striate cortex cells', *Experimental Brain Research* **52**(2), 235–247.
- Hill, J. (1981) 'On the solution of reaction-diffusion equations', *IMA Journal of Applied Mathematics* **27**(2), 177–194.
- Hines, M. L. & Carnevale, N. T. (1997) 'The neuron simulation environment', *Neural computation* **9**(6), 1179–1209.
- Holmes, W. R. & Rall, W. (1992) 'Estimating the electrotonic structure of neurons with compartmental models', *Journal of Neurophysiology* **68**(4), 1438–1452.
- Keener, J. P. (2000) 'Propagation of waves in an excitable medium with discrete release sites', *SIAM Journal on Applied Mathematics* **61**(1), 317–334.
- Keener, J. & Sneyd, J. (1998) Mathematical Physiology, Springer-Verlag, NY.
- Keizer, J., Smith, G. D., Ponce-Dawson, S. & Pearson, J. E. (1998) 'Saltatory propagation of Ca<sup>2+</sup> waves by Ca<sup>2+</sup> sparks', *Biophysical journal* **75**(2), 595–600.
- Kobayashi, T., Kuriyama, R. & Yamazaki, T. (2021) 'Testing an explicit method for multi-compartment neuron model simulation on a gpu', *Cognitive Computation* **15**, 1–14.
- Koizumi, A. & Poznanski, R. R. (2015) 'Does heterogeneity of intracellular Ca<sup>2+</sup> dynamics underlie speed tuning of direction-seelctive responses in starburst aamcrine cells?', *Journal of Integrative Neuroscience* **14**(4), 503–519.
- Kuba, K. & Takeshita, S. (1981) 'Simulation of intracellular Ca<sup>2+</sup> oscillation in a sympathetic neurone', *Journal of Theoretical Biology* **93**, 1009–1031.
- Lindsay, A., Lindsay, K. & Rosenberg, J. (2007) 'New concepts in compartmental modelling', *Computing and Visualization in Science* **10**, 79–98.
- Lions, J. L. (1971) Optimal control of systems governed by partial differential equations, Vol. 170, Springer.
- Martinez, L. M., Alonso, J.-M., Reid, R. C. & Hirsch, J. A. (2002) 'Laminar processing of stimulus orientation in cat visual cortex', *The Journal of Physiology (London)* **540**(1), 321–333.

- Merkulyeva, N., Lyakhovetskii, V. & Mikhalkin, A. (2025) 'Anisotropy of the orientation selectivity in the visual cortex area 18 of cats reared under normal and altered visual experience', *European Journal of Neuroscience* **61**(2), e70004.
- Movshon, J. A. (1975) 'The velocity tuning of single units in cat striate cortex.', *The Journal of Physiology (London)* **249**(3), 445–468.
- Murphy, P. & Sillito, A. (1986) 'Continuity of orientation columns between superficial and deep laminae of the cat primary visual cortex.', *The Journal of Physiology (London)* **381**(1), 95–110.
- Neymotin, S. A., McDougal, R. A., Sherif, M. A., Fall, C. P., Hines, M. L. & Lytton, W. W. (2015) 'Neuronal Ca<sup>2+</sup> wave propagation varies with changes in endoplasmic reticulum parameters: a computer model', *Neural Computation* **27**, 898–924.
- Scholl, B., Tan, A. Y., Corey, J. & Priebe, N. J. (2013) 'Emergence of orientation selectivity in the mammalian visual pathway', *Journal of Neuroscience* **33**(26), 10616–10624.
- Thul, R., Smith, G. & Coombes, S. (2008) 'A bidomain threshold model of propagating calcium waves', *Journal of Mathematical Biology* **56**(4), 435–463.
- Tuckwell, H. C. (1988) Introduction to Theoretical Neurobiology, vol 1, Linear Cable Theory and Dendritic Structure, Cambridge University Press, New York.
- Volgushev, M., Pei, X., Vidyasagar, T. & Creutzfeldt, O. (1993) 'Excitation and inhibition in orientation selectivity of cat visual cortex neurons revealed by whole-cell recordings in vivo', *Visual Neuroscience* **10**(6), 1151–1155.